Title: Enhancing Cardiovascular Monitoring: A Non-Linear Model for Characterizing RR Interval Fluctuations in Exercise and Recovery.

Authors: Matías Castillo-Aguilar[1], Diego Mabe-Castro[1,2], David Medina[4,5], Cristian Núñez-Espinosa[1,3]*.

[1] Centro Asistencial Docente e Investigación (CADI-UMAG), Universidad de Magallanes, Punta Arenas, Chile.
[2] Departamento de Kinesiología, Universidad de Magallanes, Punta Arenas, Chile.
[3] Escuela de Medicina, Universidad de Magallanes, Punta Arenas, Chile.
[4] Departamento de Ingeniería en Computación, Universidad de Magallanes, Punta Arenas, Chile.
[5] Centre for Biotechnology and Bioengineering, CeBiB, Universidad de Chile, Santiago, Chile.

Correspondence:

Cristian Núñez-Espinosa, Escuela de Medicina, Universidad de Magallanes, Punta Arenas, Chile. Centro Asistencial de Docencia e Investigación CADI-UMAG, Chile. e-mail: cristian.nunez@umag.cl. Address: Avenida Bulnes 01855, Box 113-D. Phone: +56 61 2201411.

Abstract

This work aimed to develop and validate a novel non-linear model to characterize RR interval (RRi) time-dependent fluctuations throughout a rest-exercise-recovery protocol, offering a more precise and physiologically relevant representation of cardiac autonomic responses than traditional HRV metrics or linear approaches. Using data from a cohort of 272 elderly participants, the model employs logistic functions to capture the non-stationary and transient nature of RRi time-dependent fluctuations, with parameter estimation achieved via Hamiltonian Monte Carlo. Sobol sensitivity analysis identified baseline RRi (α) and recovery proportion (c) as the primary drivers of variability, underscoring their critical roles in autonomic regulation and resilience. Validation against real-world RRi data demonstrated robust model performance (R^2 = 0.868, $CI_{95\%}$[0.834, 0.895] and Root Mean Square Error [RMSE] = 32.6 ms, $CI_{95\%}$[30.01, 35.77]), accurately reflecting autonomic recovery and exercise-induced fluctuations. By advancing real-time cardiovascular assessments, this framework holds significant potential for clinical applications in rehabilitation and cardiovascular monitoring in athletic contexts to optimize performance and recovery. These findings highlight the model's ability to provide precise, physiologically relevant assessments of autonomic function, paving the way for its use in personalized health monitoring and performance optimization across diverse populations.

Keywords: Heart Rate Variability, Exercise Physiology, Autonomic Nervous System, Cardiovascular System, Models, Theoretical, Logistic Models.

Introduction

The human cardiovascular system exhibits intricate dynamic responses to physical exertion, reflecting the complex interplay between the autonomic nervous system (ANS) and cardiac function. Understanding these time-dependent fluctuations is crucial for assessing physiological adaptation to exercise, optimizing athletic performance, and evaluating cardiovascular health[1–3]. R-R intervals (RRi), representing the beat-to-beat time intervals between successive heartbeats, provide a direct, high-resolution reflection of cardiac electrical activity. Unlike aggregated measures of heart rate variability (HRV), which summarize autonomic activity over longer periods and can mask transient fluctuations, RRi analysis offers a granular, beat-to-beat perspective on autonomic modulation during exercise and recovery[4–7].

This granular perspective is particularly relevant in dynamic exercise scenarios, where rapid shifts in autonomic balance occur, and in specific populations such as older adults, where age-related changes in autonomic function may influence cardiac responses[2,3,8]. Analyzing RRi allows for examining immediate cardiac responses to exercise-induced stress, providing valuable insights into the efficiency and adaptability of the cardiovascular system.

While many studies have investigated cardiovascular responses to exercise using quasi-stationary protocols, simplifying analysis by minimizing non-stationarities[9,10], these approaches may not fully capture physiological responses' dynamic and continuous nature during real-world activities. Although traditional linear methods like time-series analysis and linear regression have been employed to model RRi behavior[11], they often fall short in capturing the complex, non-linear time-dependent fluctuations of RRi transitions, particularly during periods of intense exertion and the subsequent recovery phase[12]. This limitation is significant because the ANS undergoes rapid and non-linear shifts between parasympathetic withdrawal and sympathetic activation during exercise, resulting in intricate RRi fluctuations that linear models cannot adequately represent by their nature[13]. These rapid autonomic adjustments, including vagal tone and sympathetic outflow changes, contribute to the non-linear patterns observed in RRi data[4,5]. Consequently, these simplified

models may miss critical physiological information related to cardiovascular adaptation, such as the speed and extent of recovery[14].

Model-based approaches, particularly those employing exponential functions, have been widely used to estimate heart rate and RRi recovery time constants after exercise[15–20]. While these models provide valuable insights into recovery kinetics, they often focus on specific phases of the exercise-recovery cycle. They may not fully capture the continuous transitions in RRi from rest to exercise and back to baseline. Furthermore, these models often rely on simplifying assumptions about the underlying physiological mechanisms, which may limit their ability to represent individual variability across different exercise intensities and populations accurately. Other models, like advanced non-linear approaches, have been developed to address the limitations of linear methods like decision tree-based ensemble algorithms and convolutional neural networks[21–23]. More advanced techniques, such as non-linear mode decomposition[24,25], dynamical modeling[26,27], and the explicit consideration of non-autonomous dynamics[28,29], have also been applied to analyze physiological time series.

However, many of these existing non-linear models' lack of a direct link to underlying physiological processes is a significant limitation. While they may provide a better fit to the observed data, they often lack clear physiological interpretability, limiting their clinical utility and hindering a deeper understanding of the mechanisms driving RRi changes[30–32]. Furthermore, few models are designed to capture the continuous, beat-to-beat transitions in RRi throughout the entire rest-exercise-recovery cycle while simultaneously providing physiologically meaningful parameters that can explain individual variability across diverse exercise intensities, durations, and populations[33]. This gap hinders a comprehensive understanding of how individuals adapt to exercise and how these adaptations might differ based on age, fitness level, or underlying health status. For example, understanding how RRi time-dependent fluctuations differ between trained athletes and sedentary individuals during and after exercise could provide valuable insights for personalized training programs and rehabilitation strategies.

Therefore, this paper introduces a novel non-linear model designed to characterize the continuous RRi transitions from rest to exercise and recovery. This model aims to address

the limitations of existing approaches by (1) accurately capturing the non-linear time-dependent fluctuations of RRi fluctuations throughout the entire rest-exercise-recovery cycle, providing a more complete picture of cardiovascular responses to exercise, and (2) providing physiologically interpretable parameters that reflect the underlying autonomic mechanisms, allowing for a more mechanistic understanding of individual adaptations. By focusing on these key aspects, this model offers a more detailed and physiologically relevant understanding of cardiovascular adaptation to exercise compared to traditional HRV metrics, with potential applications in personalized exercise prescription, performance monitoring, and clinical assessment of cardiovascular health.

Methods

Data collection and preprocessing

To further assess the proposed model's performance, real-world RRi data were analyzed in addition to the synthetic data generated through simulation. The dataset consisted of 272 participants who underwent a validated exercise protocol encompassing rest, exercise, and recovery phases within a single, continuous measurement session[2].

Subjects

Participants were recruited from a local community. Subjects were included if (i) they were aged 60 years or older; (ii) were permanently residing in the Magallanes and Chilean Antarctic region; (iii) had a percentage greater than 60% on the Karnofsky Performance Status Scale, which allowed us to work with older people who had a state of autonomy necessary to carry out the study tests; (iv) absence of the following diagnosis: diabetic neuropathy; use of pacemakers; clinical depression; cognitive or motor disability; and dementia. The exclusion criteria were: (i) consumption of beta-blockers during the study, (ii) taking drugs or stimulant substances within 12 hours before the cardiac assessment, and (iii) having some degree of motor disability that prevented participants from moving around. No participants met the exclusion criteria. This dataset was derived from a cohort participating in the FONDECYT Project No. 11220116, funded by the Chilean National Association of Research and Development (ANID). Ethical approval was granted by the

Ethics Committee of the University of Chile (ACTA No. 029-18/05/2022) and the Ethics Committee of the University of Magallanes (No. 008/SH/2022).

Exercise protocol

The exercise protocol consisted of the continuous measurement of RRi before, during, and immediately after the 2-minute step test, which is a part of the Senior Fitness Test protocol[34]. This functional cardiorespiratory test required each subject to march in place as many times as possible for 2 minutes. The participants were monitored throughout the assessment using cardiovascular measures (i.e., heart rate and blood pressure) to prevent adverse events during the exercise protocol. The evaluation protocol was estimated to last approximately 20 minutes for each subject. None of the participants expressed discomfort during the evaluation. Continuous heart rate data, including RRi, were collected using the Polar Team2 system (Polar®) application, capable of capturing dynamic fluctuations associated with varying exercise intensities and recovery.

Preprocessing of RRi data

Preprocessing steps were conducted to remove artifacts and ectopic heartbeats, with less than 3% of data excluded following established guidelines[35]. The preprocessed RRi data were then aggregated into time intervals to facilitate analysis, allowing the examination of acute exercise responses and post-exercise recovery patterns.

This real-world dataset provided a critical context for validating the model's predictive capability against observed physiological responses, offering a robust foundation for understanding RRi time-dependent fluctuations under physical activity conditions.

Parameter Estimation

Parameter estimation was performed using Hamiltonian Monte Carlo (HMC) with the No-U-Turn Sampler (NUTS) to explore the parameter space[36]. The parameters α, β, c, λ, ϕ, τ, and δ were estimated by sampling from the posterior distribution, which was constructed from observed RRi data and model predictions.

The gradient of the log-likelihood function for each parameter was computed during estimation using the brms R package (v2.21.0), which employs the Stan probabilistic programming language. Convergence of the HMC chains was assessed using standard diagnostics, including R-hat values, kept below 1.01 for all parameters[37], and effective sample sizes targeted at a minimum of 1,000 for each parameter[38]. Trace plots were inspected to confirm stable mixing. These diagnostics collectively confirmed reliable posterior estimates for each parameter.

The fitting process utilized five Markov Chain Monte Carlo (MCMC) chains, each consisting of 10,000 iterations with a burn-in period of 5,000 iterations, resulting in 25,000 post-warmup samples.

To enhance the exploration of parameter space, we performed a two-stage analysis: We assessed parameter values at the individual level, which we then used to estimate population-level parameters. This hierarchical structure enables us to capture individual variability through subject-level random effects while estimating group-level effects across all parameters, thus providing estimates of subject- and population-level model parameters.

Individual-level analysis

Firstly, each subject's RRi data $\mathrm{RRi}_{i,t}$ was standardized against his mean $\mathrm{R\bar{R}i}_{\imath}$ and standard deviation S_{RRi_i} to improve convergence and exploration of the posterior distribution. The standardized RRi data $y_{i,t}$ for each time point t was computed as:

$$y_{i,t} = \frac{\mathrm{RRi}_{i,t} - \mathrm{R\bar{R}i}_{\imath}}{S_{\mathrm{RRi}_i}} \qquad (1)$$

This standardization allowed the model to focus on relative changes in RRi time-dependent fluctuations independent of individual baseline differences.

The model for each subject i was then specified in terms of standardized RRi data $y_{i,t}$:

$$y_{i,t} = \alpha_i + \frac{\beta_i}{1 + e^{\lambda_i \cdot (t - \tau_i)}} + \frac{-c_i \cdot \beta_i}{1 + e^{\phi_i \cdot (t - \tau_i - \delta_i)}} + \epsilon_{i,t} \qquad (2)$$

where α_i, β_i, c_i, λ_i, ϕ_i, τ_i, δ_i are the individual-specific model parameters and $\epsilon_{i,t} \sim \mathcal{N}(0, \sigma^2)$ is the residual error term at each time point t.

Afterwards, we transformed the estimated α and β parameters back to the original RRi scale, ensuring a physiologically meaningful interpretation. The transformation for each subject i is given by:

$$\begin{aligned} \alpha_i^{\mathrm{RRi}} &= \alpha_i \cdot S_{\mathrm{RRi}_i} + \bar{\mathrm{RRi}}_i \\ \beta_i^{\mathrm{RRi}} &= \beta_i \cdot S_{\mathrm{RRi}_i} \end{aligned} \qquad (3)$$

Group-level analysis

After obtaining the posterior distribution for each subject's parameters, each parameter's mean (θ^{obs}) and standard error (ϵ) were calculated. These estimates were then used as input data to create a univariate hierarchical model, capturing variability at both the subject and group levels. The modeling process is described as follows:

For each subject i, we estimated an interdependent stochastic process in which the true parameter $\theta_{k,i}$, with $k \in \{\alpha, \beta, c, \lambda, \phi, \tau, \delta\}$ with their corresponding standard error $\epsilon_{k,i}$ was used to model the observed parameter $\theta_{k,i}^{\mathrm{obs}}$ as:

$$\theta_{k,i}^{\mathrm{obs}} \sim \mathcal{N}\left(\theta_{k,i}, \epsilon_{k,i}\right) \qquad (4)$$

Then, the true parameter $\theta_{k,i}$ was further modeled as:

$$\theta_{k,i} \sim \mathcal{N}\left(\mu_k + b_{k,i}, \sigma_k^2\right) \qquad (5)$$

where μ_k is the group-level mean for parameter k, $b_{k,i}$ represents the subject-level random effect for the subject i on parameter k and σ_k^2 is the residual variance for the parameter k. The subject-level effects $b_{k,i}$ were assumed to be distributed as $b_{k,i} \sim \mathcal{N}(0, \sigma^2)$, with σ being the standard error of the subject-level effect.

Model Performance

The primary statistical performance metrics, estimated for each subject, included R^2, root mean square error (RMSE), and mean absolute percentage error (MAPE), estimated for

each subject. Bootstrap resampling across each metric was performed to estimate the mean performance of the model and corresponding quantile-based 95% CI.

Also, residual analysis were conducted to evaluate the model's accuracy in capturing RRi time-dependent fluctuations. Residuals were defined as the difference between observed and predicted RRi values. These residuals were analyzed for temporal structure and partial autocorrelation to ensure that no systematic patterns remained in the errors. This indicates that the model has sufficiently captured the underlying time-dependent fluctuations of the RRi response to exercise.

Model parameters sensitivity

Once a model that described RRi behavior in response to exercise was obtained, an assessment of the proportion of the variance explained by each model parameter was then computed.

We implemented a Sobol sensitivity analysis using Monte Carlo simulations to assess the sensitivity of model parameters influencing RRi over time. Sobol index (S_{ind}) provide a measure of the proportion of the contribution of each parameter to the variance in RRi at each time point, and it was selected for its robustness in handling non-linear and non-monotonic relationships, which are intrinsic to RRi time-dependent fluctuations in response to exercise[39].

To compute S_{ind}, 1000 Monte Carlo simulations were conducted, each involving 1000 randomly sampled parameter sets (1,000,000 model runs). For each set of parameters, RRi were calculated at each time point t across a range from 0 to 20 minutes at intervals of 0.1 minutes. The 95% CI parameter values estimated from HMC-NUTS were then used as input ranges for S_{ind} computation. Finally, the mean values of S_{ind} over the 20-minute time span for each model parameter were estimated and reported, with their corresponding 95% CI using a normal approximation based on estimated standard errors (SE).

Results

Problem characterization

RRi time-dependent fluctuations in response to exercise tend to follow a U-shaped form. The initial decrease in RRi is associated with exercise onset and an increased heart rate. After exercise cessation, an opposite increase in RRi is observed, associated with the cardiovascular recovery phase. In both cases, the drop and recovery phases occur at different rates; some individuals experience a quick recovery in RRi after exercise; however, in some others, this slope is less steep. Additionally, the new baseline reached following exercise cessation is often below the RRi baseline before exercise.

These hallmarks of RRi time-dependent fluctuations in response to exercise highlight the complex and non-linear behavior of the cardiovascular response in the context of rest and exercise conditions. Figure 1 shows an example of RRi record data.

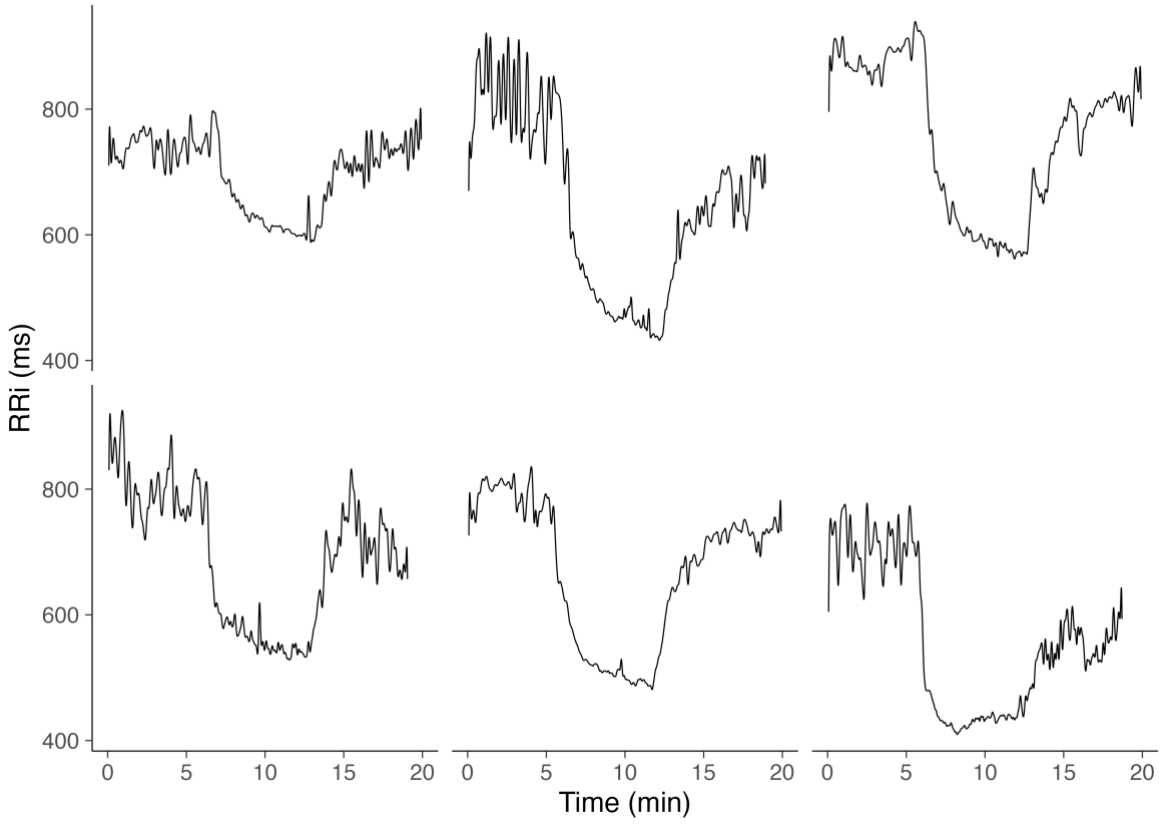

Figure 1. Example data of RRi recordings of 6 subjects over a 20-minute rest-exercise-

recovery protocol in a sample of elderly individuals. The subject-level data shows the inter-individual variability of RRi time-dependent fluctuations in response to exercised-induced cardiovascular stress, with similar behavior and recovery trajectories over time.

Model construction

The process of deriving the final equation for modeling RRi fluctuations was guided by an iterative exploration of mathematical functions capable of capturing the observed time-dependent fluctuations. Initially, exponential and logarithmic functions were considered due to their simplicity and broad applicability in describing temporal changes. Exponential functions were hypothesized to capture the rapid initial adaptations of RRi post-exercise onset. In contrast, logarithmic functions were explored for their capacity to describe asymptotic behaviors observed in some physiological variables.

However, neither approach successfully reproduced the non-linear and bidirectional nature of the RRi fluctuations. While effective at modeling monotonic decay or growth, exponential functions could not account for the observed sigmoidal transitions. Similarly, logarithmic functions, with their inherent monotonicity, failed to represent the plateauing behavior seen in real-world data.

We shifted to logistic functions to address these limitations, which inherently model sigmoidal transitions. Logistic functions introduce parameters for growth rate and inflection point, allowing for precise control over the shape and timing of the transition between dynamic states. By using two coupled logistic functions, one representing the initial decrease in RRi and a second inverted logistic function describing the recovery phase, we achieved a model structure that could flexibly reproduce the observed non-linear variations.

This approach provided a biologically plausible representation, with parameters that directly correspond to identifiable physiological features, such as the rate of adaptation and recovery, the time to peak response, and the extent of deviation from baseline. The logistic function framework emerged as the optimal solution after systematic testing and evaluation against empirical data, ensuring that the model accurately captured the qualitative and quantitative aspects of RRi time-dependent fluctuations.

The mathematical model proposed to characterize the RRi response to exercise and recovery is defined by Equation 6.

$$\mathrm{RRi}(t) = \alpha + \frac{\beta}{1 + e^{\lambda(t-\tau)}} + \frac{-c \cdot \beta}{1 + e^{\phi(t-\tau-\delta)}} \qquad (6)$$

This model includes two logistic functions representing the RRi time-dependent fluctuations across exercise and recovery phases. The first logistic term models the decrease in RRi during exercise, where the parameter β denotes the magnitude of this decline. The rate of decrease is governed by λ, while τ represents the onset of the RRi decrease or the time the physiological shift begins.

The second logistic term accounts for RRi recovery post-exercise. Here, c scales the magnitude of recovery relative to the initial decline represented by β, capturing the proportion of the decline regained during recovery. The rate at which RRi returns to baseline is controlled by ϕ, and δ indicates the lag following the cessation of exercise, marking the beginning of recovery.

Additionally, the time-dependent fluctuations of RRi in response to physical exertion can be represented as a linear combination of a baseline RRi α and two logistic functions denoted as $f_1(t)$ and $f_2(t)$. The function $f_1(t)$ models the initial decay in RRi following the initiation of exercise while $f_2(t)$ characterizes the recovery phase after exercise cessation.

Essentially, the fundamental structure of both logistic functions can be expressed as:

$$f(t) = \frac{a_1}{1 + e^{a_2(t-a_3)}} \qquad (7)$$

In this equation, a_1 represents the asymptotic value the logistic function approaches, which can be either positive (indicating an increase) or negative (indicating a decrease). For $f_1(t)$, this parameter is specified as β, indicating the absolute change in RRi at the onset of exercise. In contrast, for $f_2(t)$, a_1 is parametrized as $-c \cdot \beta$, where c denotes the proportion of change relative to the initial drop indicated by β. This parametrization ensures that, after the initial decline, the second logistic function facilitates the return of RRi toward the baseline value α.

The parameter a_2 defines the rate at which the specified increase or decrease occurs. This rate parameter is expressed on a logarithmic scale; to convert it to a percentage change per unit of time, it can be scaled as $1 - \exp(a_2)$.

The parameter a_3 serves as an activation threshold, causing the value within the exponential function, and consequently, the value in the denominator, to increase significantly until reaching a_3. Beyond this point, the denominator approaches 1, allowing the logistic function to attain the asymptotic level determined by the numerator. Figure 2 illustrates the behavior of the model constituents.

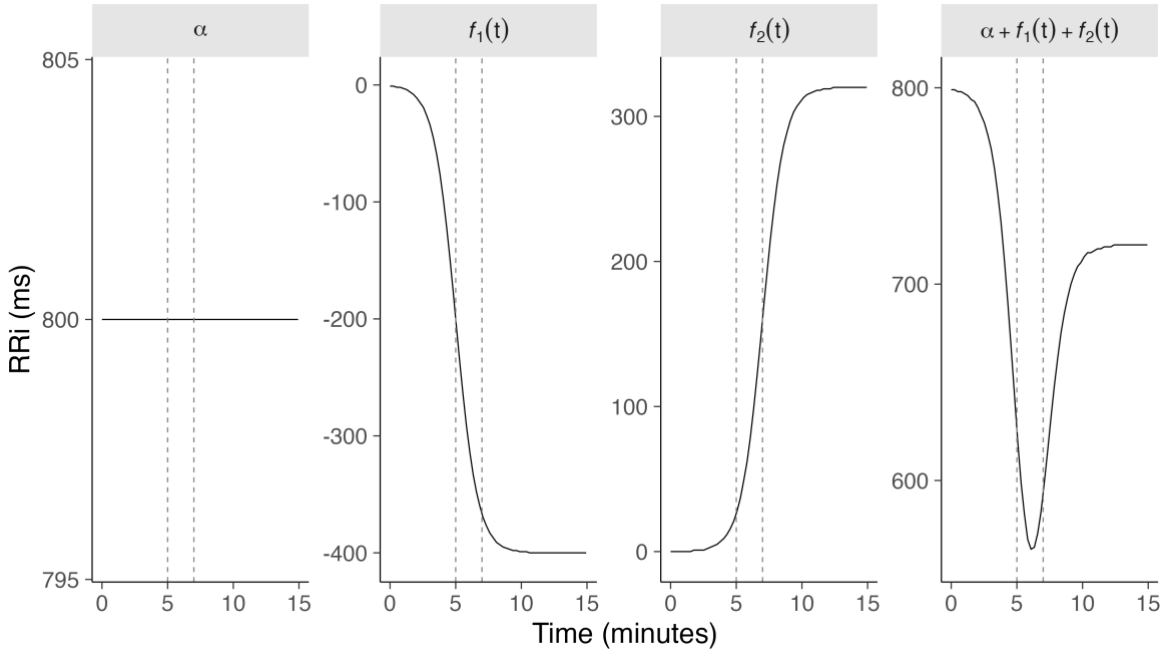

Figure 2. The RRi time-dependent fluctuations in response to exercise are expressed as a linear combination of model constituents based on the baseline RRi α and two logistic functions, denoted $f_1(t)$ and $f_2(t)$, respectively. The vertical dashed lines represent the time at which the exercise and recovery onset given by $\tau = 5$ and $\delta = 2$.

Sample characteristics

The sample used to assess RRi time-dependent fluctuations consists of 272 subjects selected from a local community of elderly individuals. The sample characteristics can be seen in Table 1

Characteristic	Overall	Female	Male
Sex	—	217 (79.8%)	55 (20.2%)
Age	71.14 ± 6.03	70.73 ± 6.27	72.73 ± 4.7
SBP (mm hg)	130.23 ± 17.07	129.58 ± 17.37	132.8 ± 15.69
DBP (mm hg)	77.1 ± 9.58	76.68 ± 9.83	78.75 ± 8.4
MAP (mm hg)	94.81 ± 10.69	94.31 ± 10.95	96.76 ± 9.45
PP (mm hg)	53.14 ± 14.07	52.9 ± 14.26	54.05 ± 13.38
BMI	30.66 ± 5.43	30.7 ± 5.64	30.53 ± 4.53
Weight (kg)	75.06 ± 14.23	73.88 ± 14.09	79.69 ± 13.95
Height (cm)	156.56 ± 9.18	155.29 ± 8.46	161.55 ± 10.24

Table 1. Sample characteristics from which continuous RRi monitoring data was collected during the rest-exercise-rest protocol. Data is presented as Mean ± standard deviation (SD). SBP, systolic blood pressure; DBP, diastolic blood pressure; MAP, mean arterial pressure; PP, pulse pressure; BMI, body mass index.

An initial graphical exploration of RRi time-dependent fluctuations (see Figure 3) indicates a clear drop in RRi around the 5-7 minutes, associated with exercise-induced cardiovascular stress. However, greater variability across individuals in post-exercise recovery can be observed.

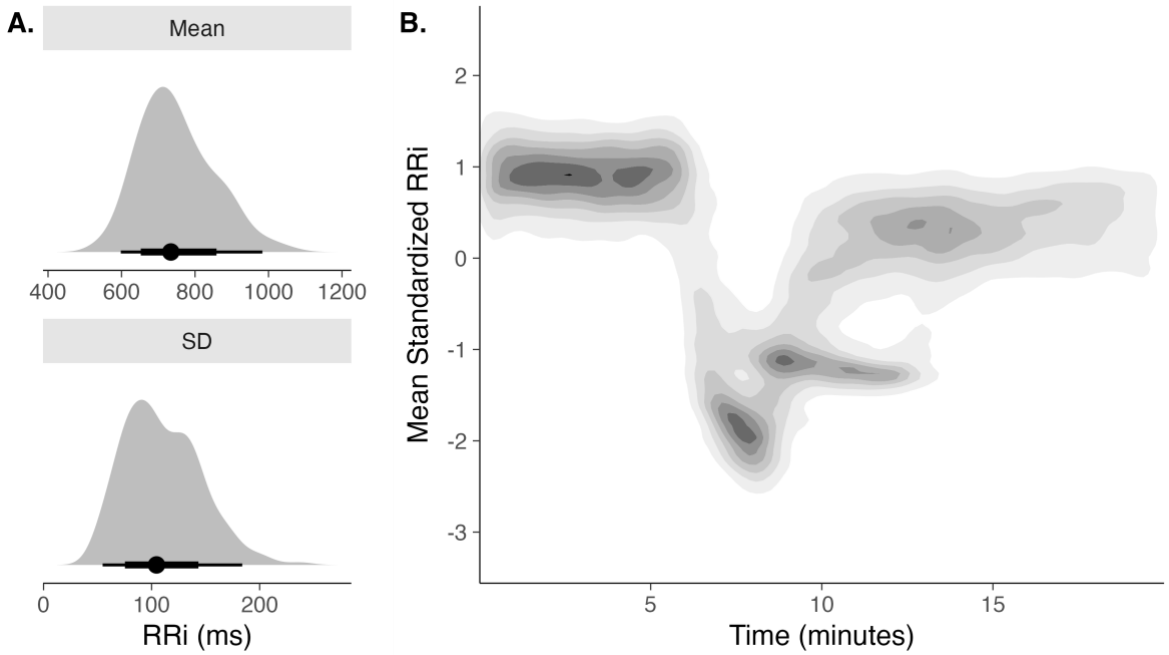

Figure 3. (A) Mean and SD from each subject's RRi recordings were used for the standardization process. (B) 2D kernel density of standardized RRi dynamics over time from a sample of individuals subjected to the rest-exercise-rest protocol. Darker colors indicate greater probability density. The contrary can be said about lighter colors.

Parameter estimation

Priors

Given the parameters that reproduced the observed RRi patterns in exercise and rest conditions, priors were chosen based on physiological constraints and the graphical visualization of standardized RRi data. Hence, ensuring the identifiability of model parameters by constraining the parameter space to plausible values to improve model convergence and parameter exploration. The prior distributions were defined as follows:

$$\begin{aligned} \alpha &\sim \mathcal{N}(1,0.5) \\ \beta &\sim \mathcal{N}(-2.5,0.5) \text{ with } \beta \leq 0 \\ c &\sim \mathcal{N}(0.8,0.2) \text{ with } c \geq 0 \\ \lambda &\sim \mathcal{N}(-2,0.5) \text{ with } \lambda \leq 0 \\ \phi &\sim \mathcal{N}(-2,0.5) \text{ with } \phi \leq 0 \\ \tau &\sim \mathcal{N}(5,0.5) \text{ with } \tau \geq 0 \\ \delta &\sim \mathcal{N}(5,0.5) \text{ with } \delta \geq 0 \end{aligned} \qquad (8)$$

Simulated standardized RRi time-dependent fluctuations based on prior parameter distributions are shown in Figure 4.

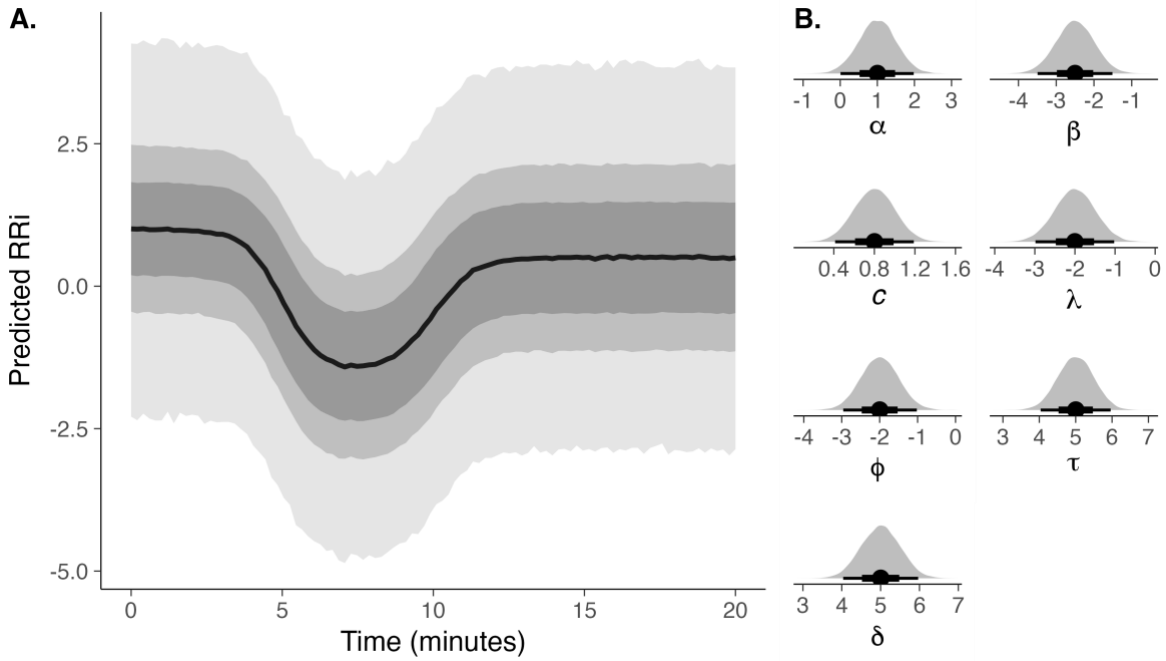

Figure 4. (A) Simulated standardized RRi time-dependent fluctuations based on prior parameter distributions, illustrating predicted RRi responses to exercise. Shaded areas represent 95%, 80%, and 60% quantile CI, offering insight into expected physiological variability across parameters. (B) Prior distributions and 95% CI were used to generate predictions based on physiological constraints and graphical visualization of standardized RRi data.

Parameter estimates

Once subject-level RRi data was fitted using the proposed model in Equation 2, a population-parameter value was estimated based on the proposed group-level methodology. The estimated parameter values can be seen in Table 2

Parameter	Estimate[1]	SE[1]	Lower[2]	Upper[2]
α	861.78	5.73	850.57	872.85
β	-345.49	7.41	-359.81	-330.97
c	0.84	0.01	0.82	0.86

Parameter	Estimate[1]	SE[1]	Lower[2]	Upper[2]
λ	-3.05	0.06	-3.16	-2.94
ϕ	-2.60	0.06	-2.71	-2.48
τ	6.71	0.05	6.61	6.81
δ	3.24	0.10	3.05	3.44
σ	27.57	0.57	26.45	28.70

Table 2. Population-parameter values estimated from group-level analysis. [1] Estimates and SE are computed as the posterior distribution's median and median absolute deviation, respectively; [2] Lower and Upper bounds from the quantile-based $CI_{95\%}$ of the posterior distribution.

In Figure 5, the model parameter's posterior distribution can be observed.

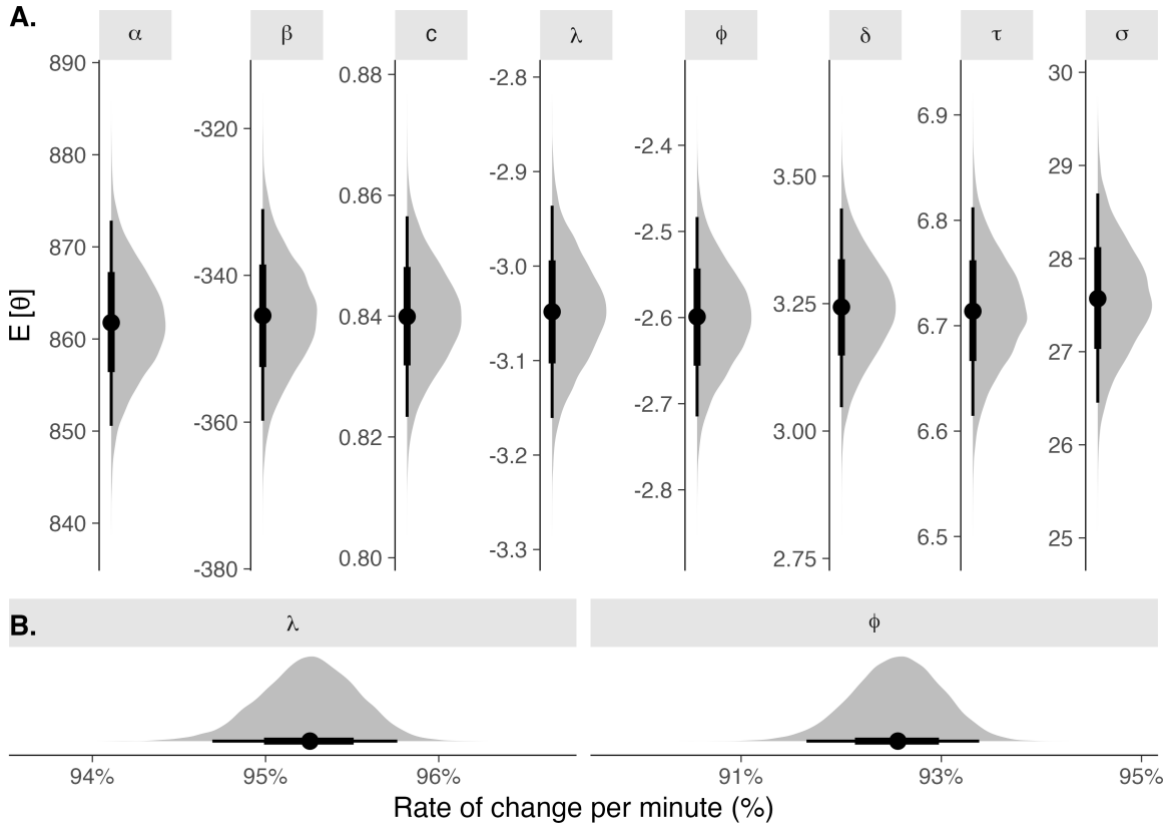

Figure 5. (A) Posterior probability distributions of the expectation for each population-

parameter estimate ($E[\theta]$) with quantile-based 95% CI. (B) Transformed rate parameters into a percentage scale using the $1 - \exp(\theta)$ transformation.

Model evaluation

Model performance

Estimated through bootstrapped resampling, relative statistical performance metrics suggest that the model tends to deviate by 3.4% ($CI_{95\%}$[3.06, 3.81]) from the observed RRi data. This is equivalent to a 32.6 ms in the RRi scale ($CI_{95\%}$[30.01, 35.77]). Additionally, the bootstrapped R^2 indicates that the model explains 0.868 ($CI_{95\%}$[0.834, 0.895]) of the total variance observed in RRi.

Residuals analysis showed that the estimated partial correlation function (ACF) from the model residuals indicates a correlation among non-explained errors greater than 0.1 up to the 5th lag. However, the partial ACF is significant (CI-wise) and strictly positive or negative until the second lag. Correlations among model residuals against other time indices remained insignificant (see Figure 6).

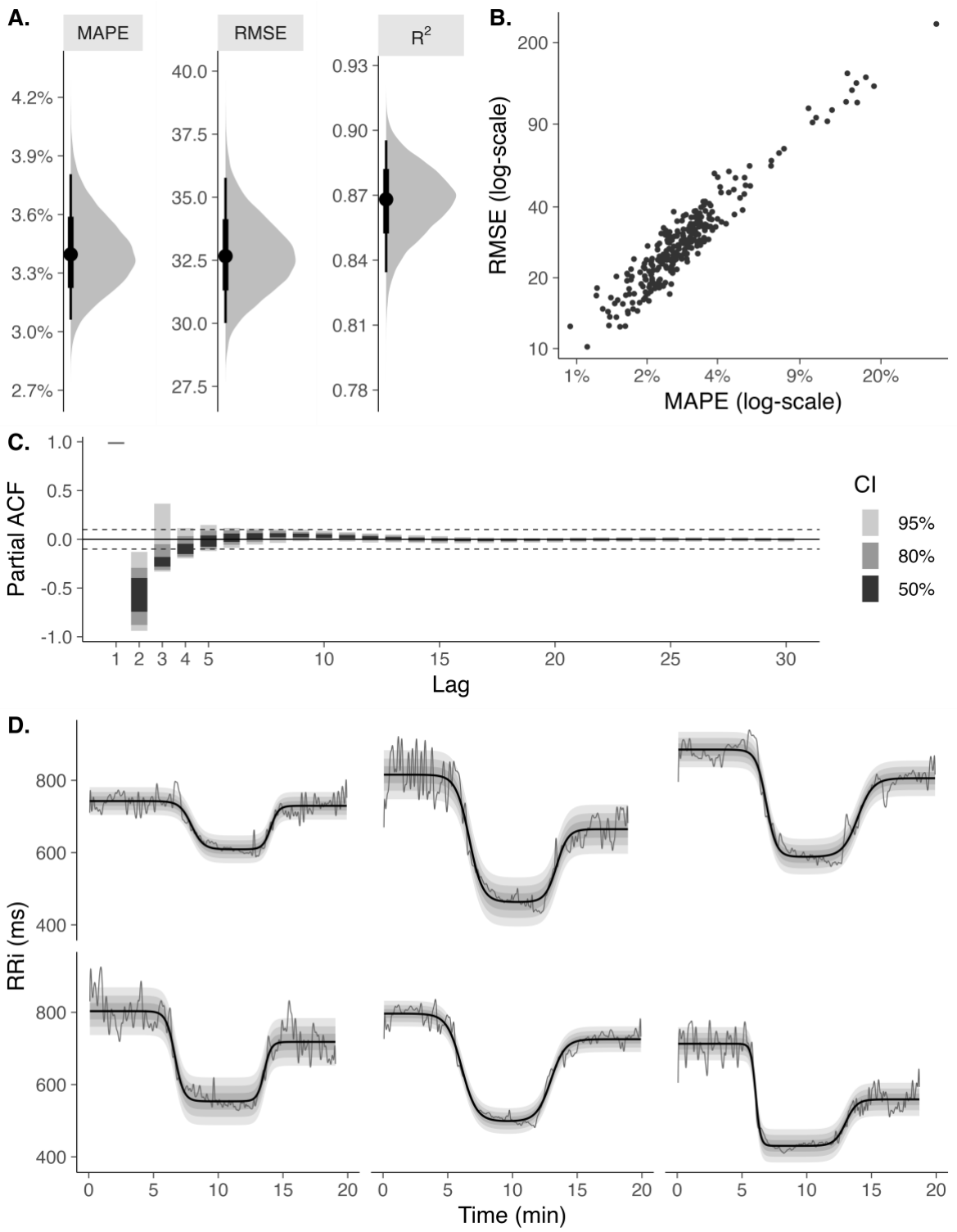

Figure 6. Individual-level performance metrics. (A) Bootstrapped MAPE and RMSE are statistical metrics of relative and absolute model deviance from observed RRi. (B) Individual-level estimates of model performance and the relationship between them. (C) Partial autocorrelation function (ACF) of model residuals with corresponding quantile-

based CI. (D) Example data with model estimates of RRi fluctuations and corresponding quantile-based CI initially displayed.

Model parameters sensitivity

Sobol sensitivity analysis reveals that the parameter α exerts the most substantial influence on the model's output, followed by parameters c and δ. In contrast, parameters β, λ, and ϕ demonstrate relatively minor effects, with some values crossing zero, indicating negligible influence within the tested parameter ranges.

Individual perturbation of each parameter highlighted that RRi time-dependent fluctuations are sensitive to the baseline RRi parameter, α. Conversely, the rate parameters for the initial decay during exercise, λ, and the recovery post-exercise, ϕ, show lower sensitivity, suggesting that they are not primary sources of variation in predicted RRi trajectories when assessed in isolation. The results of the sensitivity analysis are in Table 3.

Parameter	Estimate[1]	SE[1]	Lower[2]	Upper[2]
α	0.61329	0.01756	0.57887	0.64771
β	0.06651	0.00286	0.06090	0.07212
c	0.18939	0.00815	0.17342	0.20536
λ	0.00147	0.00007	0.00133	0.00161
ϕ	0.00160	0.00008	0.00144	0.00176
τ	0.04982	0.00172	0.04645	0.05319
δ	0.07896	0.00239	0.07428	0.08364

Table 3. Estimated S_{ind} of model parameters. [1] Estimates and SE are computed as mean and standard deviation of Monte Carlo samples, respectively. Each parameter's S_{ind} reflects a uniform variation from the 95% CIs of the estimated parameter values.

Discussion

To our knowledge, this study represents the first attempt to develop a non-linear model specifically designed to capture RRi time-dependent fluctuations continuously across a complete rest-exercise-rest protocol. Previous studies have either focused on aggregate HRV indices or utilized simplified linear or exponential models, which are insufficient to describe the complex, non-stationary transitions observed during and after exercise[40]. By employing a combination of logistic functions, our model uniquely accounts for the gradual shifts in autonomic regulation denoted by RRi time-dependent fluctuations, offering a detailed and physiologically relevant representation of cardiac dynamics. This continuous modeling framework integrates exercise-induced RRi decline and post-exercise recovery within a single unified structure, bridging a critical gap in the current literature. Such an approach advances our understanding of cardiovascular responses and opens new avenues for real-time monitoring and intervention in clinical and athletic settings.

The proposed model demonstrates a precise capacity to reproduce RRi dynamics. Its combination of logistic functions captures the key transitions of cardiac response, the initial decline during exercise, and the subsequent recovery. This design accommodates the inherent non-linearity and non-stationarity of RRi time-dependent fluctuations, overcoming the limitations of linear models and exponential functions commonly used in prior studies[8,41].

Compared to previous research, our findings align with efforts to capture nonlinear dynamics in HRV to understand cardiac responses during exercise[12]. Similarly, previous studies have shown that dynamic fluctuations in RRi can serve as critical indicators of cardiorespiratory fitness[7,8]. This supports the need for models to address the complexity of cardiovascular responses during physical stress[8]. However, while many existing models focus primarily on linear metrics or aggregate HRV measures, our study provides a high-resolution analysis of RRi time-dependent fluctuations that enhances interpretability and application across diverse fitness levels and exercise intensities. Critically, many model-based approaches, particularly those employing exponential functions, have been used to estimate time constants of heart rate and RRi recovery after exercise[15–20]. These models often focus on characterizing the recovery phase and may not capture the continuous

transitions from rest to peak exercise and subsequent recovery. Our model, by contrast, provides a unified framework for modeling the entire rest-exercise-recovery cycle, allowing for the estimation of parameters that reflect both the exercise-induced changes in RRi and the subsequent recovery dynamics. This continuous modeling approach provides a more comprehensive picture of cardiovascular response to exercise than models focusing solely on recovery kinetics.

The flexibility of the logistic components allows for physiologically interpretable parameters, such as baseline RRi (α) and recovery proportion (c), which directly correlate with intrinsic cardiac function and autonomic recovery capacity, respectively. These features position the model as a robust framework for investigating the cardiovascular system's dynamic adaptation to physical stressors. For example, prior studies have highlighted the inadequacy of linear HRV metrics in capturing transient autonomic shifts[42]; our results align with this critique, demonstrating the advantages of modeling RRi directly.

Prior studies have examined cardiorespiratory interactions using both deterministic and stochastic approaches. Deterministic models have demonstrated that respiration-driven heart rate fluctuations exhibit structured, predictable behavior, suggesting an underlying regulatory mechanism of autonomic control[43,44]. Conversely, stochastic models emphasize the role of random variability in these interactions, accounting for inherent physiological fluctuations[45]. Our non-linear model aligns with the deterministic perspective by employing logistic functions to characterize time-dependent RRi fluctuations while also incorporating inter-individual variability. Although this model does not explicitly integrate stochastic noise, it captures structured autonomic responses. Future work could explore the incorporation of stochastic elements to further enhance its applicability in more variable physiological conditions.

Unlike prior research that aggregates HRV measures or applies simple decay models, our approach directly models RRi changes, offering richer physiological insight. For instance, commonly utilized exponential decay models for post-exercise recovery are used but fail to incorporate the transition dynamics observed during exercise itself[46]. By integrating exercise and recovery phases, our model provides a more comprehensive view of autonomic regulation. Furthermore, it's important to note that the traditional

"sympathovagal balance" hypothesis, which posits a reciprocal relationship between sympathetic and parasympathetic activity, may be oversimplified, especially during exercise[9]. Recent evidence suggests that parasympathetic control can remain active even during periods of high sympathetic activation. By capturing the continuous time-dependent fluctuations of RRi, our model may provide insights into these complex interactions, potentially revealing nuances in autonomic control that are not captured by simpler models that assume a strict sympathovagal balance.

Moreover, the sensitivity of parameters such as λ (decay rate) and ϕ (recovery rate) was found to be relatively low, suggesting that the model is robust to variability in these rates while remaining sensitive to key physiological parameters (α and c). This robustness makes it suitable for individualized monitoring and population-level analyses, offering versatility in its application across different use cases.

The Sobol sensitivity analysis revealed that baseline RRi (α) and recovery proportion (c) are the primary drivers of model output variance, emphasizing their physiological importance. These findings are consistent with prior research, which identified baseline cardiac function as a determinant of cardiovascular health and recovery proportion as a marker of autonomic resilience[14].

However, the Sobol method assumes parameter independence, which may overlook interactions common in biological systems[47–49]. For example, the interplay between λ and c, which dictates the rate and magnitude of recovery, is likely critical but remains unexplored in the current framework. Future studies could explore Bayesian sensitivity analysis or variance decomposition methods that account for parameter interdependence[50,51]. Furthermore, more advanced techniques, such as non-linear mode decomposition[24,25], dynamical modeling[26,27], and the explicit consideration of non-autonomous dynamics[28,29], offer powerful tools for analyzing physiological time series. While these methods can capture complex dynamics, our model provides a more direct link to physiological interpretation through its parameters related to specific aspects of autonomic control. Future work could investigate how these approaches could be combined or compared to enhance our understanding of RRi time-dependent fluctuations.

This model demonstrates significant potential for practical applications in clinical and athletic settings. In clinical contexts, it could aid in tailoring cardiovascular rehabilitation protocols by monitoring autonomic recovery in real-time, ensuring safe and effective exercise regimens for at-risk populations[52]. This aligns with previous research, highlighting the importance of individualizing rehabilitation programs to optimize recovery[52–54].

The model could guide training strategies in athletic settings, particularly for interval training, where determining optimal recovery periods is crucial. Similar findings suggest that precise monitoring of RRi time-dependent fluctuations can prevent overtraining and enhance performance[55,56]. The model's ability to integrate real-time data from wearable devices further enhances its applicability in dynamic, uncontrolled environments, enabling field-based monitoring and feedback[57].

While the model presents substantial advances, it has limitations that warrant consideration. First, the assumption of uniform parameter sampling in sensitivity analysis, while practical, may not fully capture the variability observed in populations with extreme autonomic profiles[4]. Empirical distributions, or Bayesian priors, could improve parameter estimation and enhance the model's applicability to diverse populations[51]. Bayesian inference could be a valuable extension of this work, particularly dynamic Bayesian inference[58–60], specifically designed to model time-evolving dynamics. This approach could allow for the incorporation of prior knowledge about individual physiological characteristics and provide more robust estimates of the model parameters.

Another limitation lies in the demographic composition of the sample, which consisted exclusively of elderly individuals. While this population provides valuable insights into age-specific cardiovascular time-dependent fluctuations, the findings may not fully generalize to younger populations, whose autonomic responses to exercise and recovery differ significantly due to higher baseline vagal tone, greater cardiac plasticity, and distinct metabolic profiles[61,62]. Previous studies have demonstrated that younger individuals exhibit faster autonomic recovery and greater adaptability during physical exertion compared to older populations[62,63]. This suggests that the parameter estimates derived from this model may vary across age groups[62,63]. Future research should validate the model in more diverse cohorts, including younger adults and athletes, to ensure broader applicability and to

explore potential age-dependent modifications of the model's parameters. This would enhance its utility in clinical and athletic contexts, where age diversity is a critical factor[62,63].

Furthermore, the uneven sex ratio in our sample (79.8% female, 20.2% male) is another limitation that should be addressed in future studies. Sex differences in autonomic control have been reported[61], and this imbalance could have influenced our results. Future research should strive for a more balanced sex ratio to minimize potential bias and explore sex-specific differences in RRi time-dependent fluctuations during exercise and recovery. This study did not explicitly consider environmental and psychological factors like temperature, stress, or sleep quality. Future work could integrate these variables into the model, enhancing its robustness and applicability across varied real-world scenarios. This aligns with calls for more integrative modeling approaches in cardiovascular research[53,55,56].

Conclusion

In summary, this study presents a novel non-linear model for RRi time-dependent fluctuations, capturing the complex and transient autonomic responses during rest-exercise-recovery protocols, overcoming the limitations of traditional autonomic metrics. The model emphasizes their critical roles in reflecting autonomic regulation and resilience by identifying baseline RRi and recovery proportion as the dominant contributors to variability. Validated across a cohort of elderly participants, the model demonstrates robust performance in real-time cardiovascular assessments, offering significant potential for clinical applications such as rehabilitation and monitoring in at-risk populations and athletic contexts like fatigue management and performance optimization. While the model's applicability is currently constrained by its focus on elderly individuals, future validation in younger cohorts and under diverse environmental conditions will enhance its generalizability and utility. This work establishes a foundational framework for advancing personalized cardiovascular health monitoring and intervention.

References

1. Eser, P. *et al.* Acute and chronic effects of high-intensity interval and moderate-intensity continuous exercise on heart rate and its variability after recent myocardial infarction: A randomized controlled trial. *Annals of Physical and Rehabilitation Medicine* **65**, 101444 (2022).

2. Castillo-Aguilar, M. *et al.* Validity and reliability of short-term heart rate variability parameters in older people in response to physical exercise. *International Journal of Environmental Research and Public Health* **20**, 4456 (2023).

3. Mabe-Castro, D. *et al.* Associations between physical fitness, body composition, and heart rate variability during exercise in older people: Exploring mediating factors. *PeerJ* **12**, e18061 (2024).

4. Kristal-Boneh, E., Raifel, M., Froom, P. & Ribak, J. Heart rate variability in health and disease. *Scandinavian journal of work, environment & health* 85–95 (1995).

5. Thayer, J. F., Yamamoto, S. S. & Brosschot, J. F. The relationship of autonomic imbalance, heart rate variability and cardiovascular disease risk factors. *International journal of cardiology* **141**, 122–131 (2010).

6. Dong, J.-G. The role of heart rate variability in sports physiology. *Experimental and therapeutic medicine* **11**, 1531–1536 (2016).

7. Lundstrom, C. J., Foreman, N. A. & Biltz, G. Practices and applications of heart rate variability monitoring in endurance athletes. *International journal of sports medicine* **44**, 9–19 (2023).

8. Mongin, D. *et al.* Decrease of heart rate variability during exercise: An index of cardiorespiratory fitness. *Plos one* **17**, e0273981 (2022).

9. Storniolo, J. L., Cairo, B., Porta, A. & Cavallari, P. Symbolic analysis of the heart rate variability during the plateau phase following maximal sprint exercise. *Frontiers in physiology* **12**, 632883 (2021).

10. Porta, A. *et al.* On the relevance of computing a local version of sample entropy in cardiovascular control analysis. *IEEE Transactions on Biomedical Engineering* **66**, 623–631 (2018).

11. Lian, J., Wang, L. & Muessig, D. A simple method to detect atrial fibrillation using RR intervals. *The American journal of cardiology* **107**, 1494–1497 (2011).

12. Gronwald, T., Hoos, O. & Hottenrott, K. Effects of a short-term cycling interval session and active recovery on non-linear dynamics of cardiac autonomic activity in endurance trained cyclists. *Journal of clinical medicine* **8**, 194 (2019).

13. Boettger, S. *et al.* Heart rate variability, QT variability, and electrodermal activity during exercise. *Med sci sports exerc* **42**, 443–8 (2010).

14. Hautala, A. J., Mäkikallio, T. H., Seppänen, T., Huikuri, H. V. & Tulppo, M. P. Short-term correlation properties of r–r interval dynamics at different exercise intensity levels. *Clinical physiology and functional imaging* **23**, 215–223 (2003).

15. Imai, K. *et al.* Vagally mediated heart rate recovery after exercise is accelerated in athletes but blunted in patients with chronic heart failure. *Journal of the American College of Cardiology* **24**, 1529–1535 (1994).

16. Borresen, J. & Lambert, M. I. Autonomic control of heart rate during and after exercise: Measurements and implications for monitoring training status. *Sports medicine* **38**, 633–646 (2008).

17. Pierpont, G. L., Stolpman, D. R. & Gornick, C. C. Heart rate recovery post-exercise as an index of parasympathetic activity. *Journal of the autonomic nervous system* **80**, 169–174 (2000).

18. Pierpont, G. L. & Voth, E. J. Assessing autonomic function by analysis of heart rate recovery from exercise in healthy subjects. *The American journal of cardiology* **94**, 64–68 (2004).

19. Buchheit, M., Laursen, P. B. & Ahmaidi, S. Parasympathetic reactivation after repeated sprint exercise. *American journal of physiology-heart and circulatory physiology* **293**, H133–H141 (2007).

20. Peçanha, T., Silva-Júnior, N. D. & Forjaz, C. L. de M. Heart rate recovery: Autonomic determinants, methods of assessment and association with mortality and cardiovascular diseases. *Clinical physiology and functional imaging* **34**, 327–339 (2014).

21. Wang, J. Automated detection of atrial fibrillation and atrial flutter in ECG signals based on convolutional and improved elman neural network. *Knowledge-Based Systems* **193**, 105446 (2020).

22. Lee, H. *et al.* Real-time machine learning model to predict in-hospital cardiac arrest using heart rate variability in ICU. *NPJ Digital Medicine* **6**, 215 (2023).

23. Berrahou, N., El Alami, A., Mesbah, A., El Alami, R. & Berrahou, A. Arrhythmia detection in inter-patient ECG signals using entropy rate features and RR intervals with CNN architecture. *Computer Methods in Biomechanics and Biomedical Engineering* 1–20 (2024).

24. Iatsenko, D., McClintock, P. V. & Stefanovska, A. Nonlinear mode decomposition: A noise-robust, adaptive decomposition method. *Physical Review E* **92**, 032916 (2015).

25. Iatsenko, D., McClintock, P. V. & Stefanovska, A. Extraction of instantaneous frequencies from ridges in time–frequency representations of signals. *Signal Processing* **125**, 290–303 (2016).

26. Kralemann, B. *et al.* In vivo cardiac phase response curve elucidates human respiratory heart rate variability. *Nature communications* **4**, 2418 (2013).

27. Stankovski, T., Duggento, A., McClintock, P. V. & Stefanovska, A. Inference of time-evolving coupled dynamical systems in the presence of noise. *Physical review letters* **109**, 024101 (2012).

28. Clemson, P. T. & Stefanovska, A. Discerning non-autonomous dynamics. *Physics Reports* **542**, 297–368 (2014).

29. Lehnertz, K. Time-series-analysis-based detection of critical transitions in real-world non-autonomous systems. *Chaos: An Interdisciplinary Journal of Nonlinear Science* **34**, (2024).

30. Gronwald, T., Hoos, O., Ludyga, S. & Hottenrott, K. Non-linear dynamics of heart rate variability during incremental cycling exercise. *Research in Sports Medicine* **27**, 88–98 (2019).

31. Bacopoulou, F., Chryssanthopoulos, S., Koutelekos, J., Lambrou, G. I. & Cokkinos, D. Entropy in cardiac autonomic nervous system of adolescents with general learning disabilities or dyslexia. in *GeNeDis 2020: Genetics and neurodegenerative diseases* 121–129 (Springer, 2021).

32. Fonseca, R. X. da *et al.* Post-exercise heart rate recovery and its speed are associated with resting-reactivity cardiovagal modulation in healthy women. *Scientific Reports* **14**, 5526 (2024).

33. Kanniainen, M. *et al.* Estimation of physiological exercise thresholds based on dynamical correlation properties of heart rate variability. *Frontiers in physiology* **14**, 1299104 (2023).

34. Rikli, R. E. & Jones, C. J. *Senior Fitness Test Manual*. (Human kinetics, 2013).

35. Malik, M. Heart rate variability: Standards of measurement, physiological interpretation, and clinical use: Task force of the european society of cardiology and the north american society for pacing and electrophysiology. *Annals of Noninvasive Electrocardiology* **1**, 151–181 (1996).

36. Hoffman, M. D., Gelman, A., *et al.* The no-u-turn sampler: Adaptively setting path lengths in hamiltonian monte carlo. *J. Mach. Learn. Res.* **15**, 1593–1623 (2014).

37. Vehtari, A., Gelman, A., Simpson, D., Carpenter, B. & Bürkner, P.-C. Rank-normalization, folding, and localization: An improved r for assessing convergence of MCMC. arXiv. *arXiv preprint arXiv:1903.08008* (2019).

38. Bürkner, P.-C. brms: An R package for Bayesian multilevel models using Stan. *Journal of Statistical Software* **80**, 1–28 (2017).

39. Zhang, X.-Y., Trame, M. N., Lesko, L. J. & Schmidt, S. Sobol sensitivity analysis: A tool to guide the development and evaluation of systems pharmacology models. *CPT: pharmacometrics & systems pharmacology* **4**, 69–79 (2015).

40. Molkkari, M., Solanpää, J. & Räsänen, E. Online tool for dynamical heart rate variability analysis. in *2020 computing in cardiology* 1–4 (IEEE, 2020).

41. Silva, L. R. B. *et al.* Exponential model for analysis of heart rate responses and autonomic cardiac modulation during different intensities of physical exercise. *Royal Society Open Science* **6**, 190639 (2019).

42. Grégoire, J.-M., Gilon, C., Carlier, S. & Bersini, H. Autonomic nervous system assessment using heart rate variability. *Acta cardiologica* **78**, 648–662 (2023).

43. Lotrič, M. B. & Stefanovska, A. Synchronization and modulation in the human cardiorespiratory system. *Physica A: Statistical Mechanics and its Applications* **283**, 451–461 (2000).

44. Iatsenko, D. *et al.* Evolution of cardiorespiratory interactions with age. *Philosophical Transactions of the Royal Society A: Mathematical, Physical and Engineering Sciences* **371**, 20110622 (2013).

45. Kenwright, D., Bahraminasab, A., Stefanovska, A. & McClintock, P. The effect of low-frequency oscillations on cardio-respiratory synchronization: Observations during rest and exercise. *The European Physical Journal B* **65**, 425–433 (2008).

46. Sahoo, K. P. *et al.* Unanticipated evolution of cardio-respiratory interactions with cognitive load during a go-NoGo shooting task in virtual reality. *Computers in Biology and Medicine* **182**, 109109 (2024).

47. Harenberg, D., Marelli, S., Sudret, B. & Winschel, V. Uncertainty quantification and global sensitivity analysis for economic models. *Available at SSRN 2903994* (2017).

48. Cheng, K., Lu, Z., Wei, Y., Shi, Y. & Zhou, Y. Mixed kernel function support vector regression for global sensitivity analysis. *Mechanical Systems and Signal Processing* **96**, 201–214 (2017).

49. Herman, J. D., Kollat, J. B., Reed, P. M. & Wagener, T. Method of morris effectively reduces the computational demands of global sensitivity analysis for distributed watershed models. *Hydrology and Earth System Sciences* **17**, 2893–2903 (2013).

50. Bornn, L., Doucet, A. & Gottardo, R. An efficient computational approach for prior sensitivity analysis and cross-validation. *Canadian Journal of Statistics* **38**, 47–64 (2010).

51. Xue, W. & Zaidi, A. Bayesian sensitivity analysis for missing data using the e-value. *arXiv preprint arXiv:2108.13286* (2021).

52. Carrasco-Poyatos, M., López-Osca, R., Martínez-González-Moro, I. & Granero-Gallegos, A. HRV-guided training vs traditional HIIT training in cardiac rehabilitation: A randomized controlled trial. *GeroScience* **46**, 2093–2106 (2024).

53. Takahashi, C. *et al.* Are signs and symptoms in cardiovascular rehabilitation correlated with heart rate variability? An observational longitudinal study. *Geriatrics & Gerontology International* **20**, 853–859 (2020).

54. Rizvi, M. R., Sharma, A., Malki, A. & Sami, W. Enhancing cardiovascular health and functional recovery in stroke survivors: A randomized controlled trial of stroke-specific and cardiac rehabilitation protocols for optimized rehabilitation. *Journal of Clinical Medicine* **12**, 6589 (2023).

55. Hebisz, R. G., Hebisz, P. & Zatoń, M. W. Heart rate variability after sprint interval training in cyclists and implications for assessing physical fatigue. *The Journal of Strength & Conditioning Research* **36**, 558–564 (2022).

56. Nuuttila, O.-P., Uusitalo, A., Kokkonen, V.-P., Weerarathna, N. & Kyröläinen, H. Monitoring fatigue state with heart rate-based and subjective methods during intensified training in recreational runners. *European Journal of Sport Science* (2024).

57. Zimatore, G. *et al.* Recurrence quantification analysis of heart rate variability during continuous incremental exercise test in obese subjects. *Chaos: An Interdisciplinary Journal of Nonlinear Science* **30**, (2020).

58. Duggento, A., Stankovski, T., McClintock, P. V. & Stefanovska, A. Dynamical bayesian inference of time-evolving interactions: From a pair of coupled oscillators to networks of oscillators. *Physical Review E—Statistical, Nonlinear, and Soft Matter Physics* **86**, 061126 (2012).

59. Stankovski, T., Duggento, A., McClintock, P. V. & Stefanovska, A. A tutorial on time-evolving dynamical bayesian inference. *The European Physical Journal Special Topics* **223**, 2685–2703 (2014).

60. Lukarski, D., Stavrov, D. & Stankovski, T. Variability of cardiorespiratory interactions under different breathing patterns. *Biomedical Signal Processing and Control* **71**, 103152 (2022).

61. Castillo-Aguilar, M. *et al.* Cardiac autonomic modulation in response to muscle fatigue and sex differences during consecutive competition periods in young swimmers: A longitudinal study. *Frontiers in Physiology* **12**, 769085 (2021).

62. Garavaglia, L., Gulich, D., Defeo, M. M., Thomas Mailland, J. & Irurzun, I. M. The effect of age on the heart rate variability of healthy subjects. *PloS one* **16**, e0255894 (2021).

63. Choi, J., Cha, W. & Park, M.-G. Declining trends of heart rate variability according to aging in healthy asian adults. *Frontiers in Aging Neuroscience* **12**, 610626 (2020).

Author Contributions

Conceptualization, MC-A; Data curation, MC-A; Investigation, MC-A, DM-C; Methodology, MC-A, NMD; Supervision, CN-E; Formal analysis, MC-A; Visualization, MC-A; Writing–original draft, MC-A, CN-E, DM-C; Writing–review & editing, MC-A, CN-E, DM. All authors have read and agreed to the published version of the manuscript.

Data Availability Statement

The authors will make the data supporting this article's conclusions available without reservation. If any data is required, please request it from the corresponding author of this work.

Competing Interests Statement

The authors declare that this research was conducted without any commercial or financial relationships that could be construed as potential conflicts of interest.

Funding

This work was funded by ANID Proyecto Fondecyt Iniciación Nº11220116.